frontiers | Frontiers in Marine Science

TYPE Original Research
PUBLISHED 25 October 2023
DOI 10.3389/fmars.2023.1254450

OPEN ACCESS

EDITED BY
Andrew R. Thurber,
Oregon State University, United States

REVIEWED BY
Weichao Wu,
Shanghai Ocean University, China
Amy Renee Smith,
Bard College at Simon's Rock,
United States

*CORRESPONDENCE
Jing-Chun Feng
fengjc@gdut.edu.cn

RECEIVED 10 July 2023
ACCEPTED 12 October 2023
PUBLISHED 25 October 2023

CITATION
Liang J, Feng J-C, Kong J, Huang Y, Zhang H, Zhong S, Tang L and Zhang S (2023) Microbial communities and mineral assemblages in sediments from various habitats at the Haima Cold Seep, South China Sea. *Front. Mar. Sci.* 10:1254450. doi: 10.3389/fmars.2023.1254450

Microbial communities and mineral assemblages in sediments from various habitats at the Haima Cold Seep, South China Sea

Jianzhen Liang[1], Jing-Chun Feng[1,2]*, Jie Kong[2], Yongji Huang[2,3], Hui Zhang[1], Song Zhong[1], Li Tang[1] and Si Zhang[2,3]

[1]School of Ecology, Environmental, and Resources, Guangdong University of Technology, Guangzhou, China, [2]Southern Marine Science and Engineering Guangdong Laboratory (Guangzhou), Guangzhou, China, [3]South China Sea Institute of Oceanology, Chinese Academy of Sciences, Guangzhou, China

Cold seeps create diverse habitats in the deep sea and play an important role in the global carbon cycling. Anaerobic oxidation of methane (AOM) and biogenic mineralization are essential carbon pathways of methane and carbon transformation in cold seeps, however, the effects of habitat heterogeneity on the processes are still poorly understood. In this study, we investigated the microbial communities and mineral assemblages at distinct habitats in the Haima cold seep and their relationships with environmental factors. These habitats were classified as methane seep site (MS), seep-free faunal habitat (FH), and control site (CS). Bacterial communities were significantly different among the three habitats. *ANME-3* archaea, *Sulfurovum* bacteria, and mineralization-associated microbes (e.g., Campylobacterales) were detected in high relative abundances at ROV2. Mineralogical analysis revealed abundant calcite minerals at the seep site, indicating that authigenic carbonate minerals were formed at highly active seep. Multivariate statistical analysis demonstrated that the concentrations of SO_4^{2-}, Ca^{2+}, and Mg^{2+} were significantly correlated with the presence of calcite minerals and bacterial communities. These results suggested that AOM-accompanied authigenic carbonate formation is an important factor influencing the mineral assemblages in seep habitats. This finding improves our understanding of marine microbial carbon cycling.

KEYWORDS

microbial community, mineral assemblage, cold seep, habitat, anaerobic oxidation of methane

1 Introduction

Cold seeps are highly productive ecosystems that host thriving biomes and play an important role in global biogeochemical cycling (Offre et al., 2013; Dan et al., 2023). Seep ecosystems are typically characterized by the upward flow from deep sediments of cold fluids rich in methane and hydrogen sulfide. These fluids support diverse chemosynthetic microbial communities (Chen et al., 2022b; Feng et al., 2022a). A diverse array of seep habitats are created by different geochemical processes occurring at different locations within the cold seep area. These processes include the cycling of methane, sulfate, metal elements, and nutrients (Zhuang et al., 2019; Cao et al., 2021). Unique habitats associated with cold seeps include methane bubble seeps (Xin et al., 2022), faunal habitats (Xu et al., 2020), and carbonate rocks (Caesar et al., 2019). Although it has been shown that different types of habitats may be dominated by distinct microorganisms that provide unique ecological functions (Bowles et al., 2016), detailed knowledge of the microbiology and mineralogy of various habitats in the cold seep area remains less understood.

In seep habitats, chemosynthetic microorganisms use methane and sulfate-bearing fluids to produce metabolites and energy to support various faunal communities (Chen et al., 2022b) such as tubeworms (Lee et al., 2021), mussels (Sun et al., 2022), and clams (Ling et al., 2020). The distribution of seep faunal communities is influenced by variations in the dominant chemoautotrophic microbial taxa in seep habitats (Thomas et al., 2018). Microbial communities are controlled by environmental factors in seep habitats such as nutrient supply, and thus their metabolic activity is influenced by habitat heterogeneity (Xin et al., 2022). Sulfate-dependent anaerobic oxidation of methane (SR-AOM) induced by methanotrophic archaea (ANME) and sulfate-reducing bacteria (SRB) is a deep-sea methane sink that consumes a large fraction of methane in seafloor sediments (Niemann et al., 2006; Feng et al., 2022b). Moreover, the SR-AOM process leads to an increase in alkalinity and dissolved inorganic carbon, thereby promoting the precipitation of authigenic carbonates (Liu et al., 2020). Authigenic carbonate minerals are often indicative of methane seepage activity and constitute the most common mineral matrix in seep habitats (Pierre et al., 2017). Thus, habitat heterogeneity in cold seep areas may drive changes in microbial community structure and affect the formation of authigenic minerals.

The Haima Seep is a cold seep system recently discovered in the South China Sea (SCS), which is located in the western Qiongdong Southeast Basin. This seep system is active and at the early and middle development stage (Feng et al., 2023). Submersible surveys have revealed that the Haima seep consisted of multiple unique habitats containing faunal communities and carbonate mounds (Xu et al., 2020). Seepage bubbles, carbonate rocks, and mussel beds have been found in seep habitats, which have various habitat characteristics and distinct microbial communities. In recent years, comparative studies of different habitats in the Haima seep have revealed that the microbial composition differs significantly between habitats in active seeps and non-seep sites (Chen et al., 2022b). Methane content is a key environmental factor driving microbial community variation in these habitats (Li et al., 2021). It has been reported that cold-seep carbonates provide a record of the seepage properties, including changes in fluid source, depositional environment, and seep activity (Guan et al., 2018). A biogeochemical study has indicated that the carbonate phase in the surface sediment from Haima is predominantly high-Mg calcite, suggesting high methane fluxes, and significant AOM activity in the area (Liu et al., 2020). The carbonate minerals at Haima are mainly aragonite, calcite, and lesser amounts of dolomite, which vary greatly in mineral composition (Chen et al., 2022a). These studies have revealed the role of geochemical factors of cold seeps in driving changes in microbial communities and mineral composition. Investigating the effects of habitat heterogeneity on microbial communities and mineral composition is important for detailed assessment of carbon cycling in cold seeps.

To determine how habitat heterogeneity within a seep area shapes microbial communities and mineral characteristics, we compared the microbial communities, environmental factors, and mineral assemblages in sediments from habitats distinguished by distinct landscapes in the Haima cold seep. Sediment samples were collected from the MS, FH, and CS. Bacterial and archaeal communities were studied using 16S rRNA gene amplicon sequencing. Mineral compositions and environmental factors in the habitats were quantified using mineralogical and geochemical analyses. The goal of this study was to better understand: (i) whether intergroup differences exist among sampling sites with various habitats in the cold seep zone, (ii) correlations among microbial community structure, mineral assemblages, and environmental factors, and (iii) the signature microbes in cold seep habitats and carbonate minerals, particularly with respect to whether species associated with methane oxidation and carbonate precipitation inhabit this ecosystem.

2 Materials and methods

2.1 Study area and collection of sediment samples

Sampling was conducted during an expedition in September 2020 at the Haima cold seep area, which is located on the northern SCS continental slope (Feng et al., 2022c) (Figure 1A). Surface sediment samples (0–30 cm) in the area were collected from the seafloor to the ship by using a box corer. For subsequent experimental analyses, sediment samples were collected only in the surface 0–5 cm of the box and then immediately frozen for preservation. The sampling sites in the cold seep area were visually classified based on the presence or absence of methane bubbles in the habitats observed through the diving ROV *Haima*. Three sampling sites were selected based on distinct landscapes: a site with continuous methane bubbles and some live mussels (MS); a site without methane bubbles and with fauna such as live mussels, live conches, dead clams, and live king crabs (FH); and a site with only normal sediments and outside the active seepage (CS) (Figure 1B). Two samples (ROV1 and ROV2; water depths: 1,420

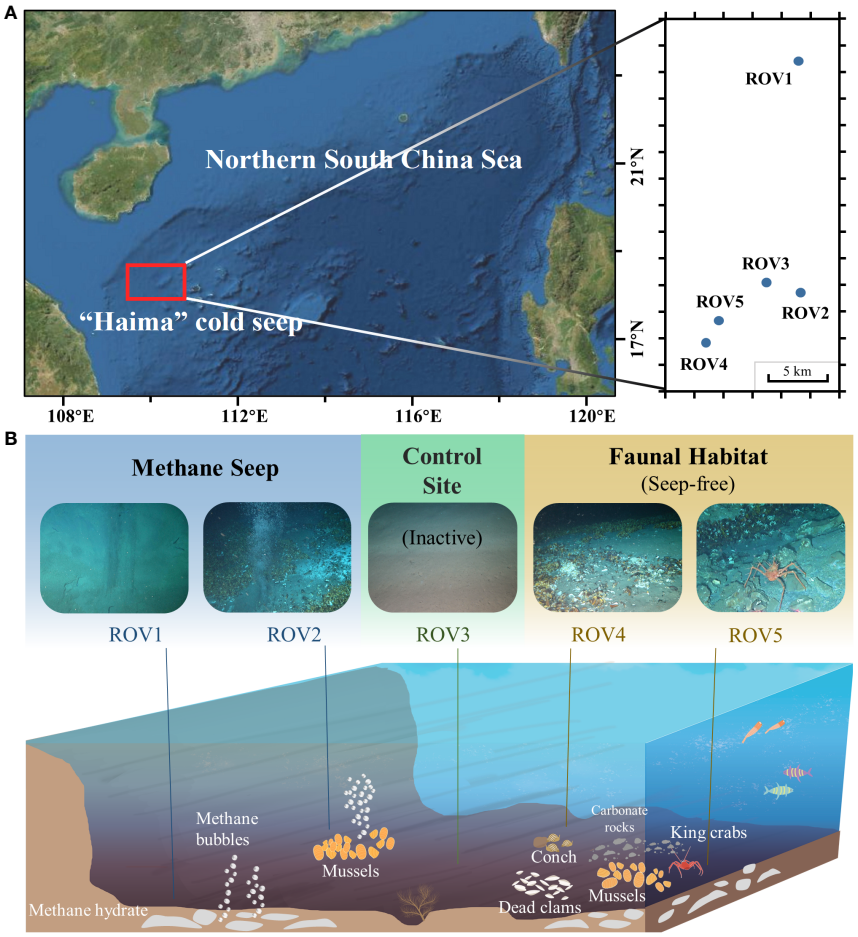

FIGURE 1
Sampling locations **(A)** and habitat features **(B)** at the MS site (ROV 1 and ROV 2), the CS site (ROV 3), and the FH site (ROV 4 and ROV 5) in the Haima cold seep area.

m and 1,384 m) were collected at the MS site, two samples (ROV4 and ROV5; water depth: 1,348 m and 1,347 m) were collected at the FH site, and one sample (ROV3; water depth: 1,378 m) was collected at the CS site. The three sampling sites of MS, CS, and FH were 1–5 km apart. Stations ROV1 and ROV2 were approximately 10 km apart at two different sites of methane seepage. In the *in-situ* observations, ROV1 had no characteristic species and low-rate methane bubbles, while ROV2 had significant mussels and methane bubbles. Based on the theory of the developmental stages of cold seeps (Feng et al., 2023), Stations ROV1 and ROV2 were in the early and early-mid stages of cold seep development, respectively. ROV5 was in the mid-late stage of non-seepage and was evidenced by live and dead mussels and some exposed hydrates. The hydrates in the ROV5 sediment were also observed in the collected samples.

2.2 Geochemical and mineralogical analyses

Salinity, temperature, and dissolved oxygen of bottom seawater were recorded by a conductivity–temperature–depth (CTD) sampler (SBE 911, Sea-Bird Electronics Co. Ltd., Bellevue, Washington, USA). Total organic carbon (TOC) and inorganic carbon (IC) in the sediments were quantified using a TOC analyzer (Shimadzu TOC-L, Kyoto, Japan) that employed catalytic combustion at 900°C (following the manufacturer's instruction). After extraction of pore waters from sediments, the samples were filtered through a 0.22 μm membrane to remove sediment and then were diluted according to the detection limit of the analyzing instrument. The anions (NO_3^- and SO_4^{2-}) were detected using ion chromatography (Thermo Fisher AQ-1200, Waltham, MA, USA) operating at 30°C (Feng et al., 2023). An AS11-HC column was used at a flow rate of 1 mL/min. The ADRS600 suppressor current was set at 120 mA, and the sample test was conducted according to the manufacturer's instructions. For quantification of the metal elements, an inductively coupled plasma-optical emission spectrometer (ICP-OES, Thermo Fisher iCAP 7000 SERIES, Waltham, MA, USA) was used to detect the concentrations of Calcium (Ca), Magnesium (Mg), Natrium (Na), and Strontium (Sr) (Feng et al., 2023). Analysis procedures followed the manufacturer's instructions.

After removing organic matter and carbonate with 10% H_2O_2 and 10% HCl (v/v), respectively, grain-size composition was

analyzed using a Laser Particle Size Analyzer (Mastersizer 3000, Malvern, UK), (Feng et al., 2022c). A 0.05 mol/l sodium metaphosphate solution was added to the samples to prevent the aggregation of fine particles before the analysis. For mineral analysis, the crystalline phases of the five sediment samples were analyzed using X-ray diffraction (XRD, D/Max-rA, Rigaku, Japan). All samples were air-dried, ground to homogenize them and run as packaged powders. The samples were scanned by XRD with Cu Kα radiation at 40 kV/45 mA over a range of 5–70° 2θ (where θ is the scan angle) (Wei et al., 2020). The results were identified using the International Center for Diffraction Data 2014. The relative quantification of phases was given in weight percent. The morphological features and element components of the samples were then characterized using scanning/transmission electron microscopy (S/TEM, Thermo Fisher Talos F200S, Waltham, MA, USA) coupled with energy dispersive spectroscopy (EDS) (Marlow et al., 2021).

2.3 DNA extraction, PCR, and 16S rRNA gene sequencing

The microbial community compositions in the Haima area were explored using an Illumina high-throughput sequencing approach (Kong et al., 2023). The total genomic deoxyribonucleic acid (DNA) of the microbes was extracted from 0.5 g sediment following the Zhou method (Zhou et al., 1996). Sediments were freeze-thawed in a high-salt extraction buffer containing hexadecyltrimethylammonium bromide (CTAB) and 1.5 M NaCl. Samples were then treated with sodium dodecyl sulfate (SDS) and proteinase K, and extracted with chloroform-isoamyl alcohol. The purity and quality of extracted DNAs were evaluated using a NanoDrop ND-2000 spectrophotometer (Thermo Fisher, Waltham, MA, USA) and agarose gel electrophoresis. The DNA concentrations were measured using a Qubit 3.0 Fluorometer (Life Technologies, CA, USA).

Polymerase chain reaction (PCR) amplification of the 16S rRNA gene of the V3-V4 region was performed using the primers bacteria (341F: 5′-CCTACGGGNGGCWGCAG-3′/806R: 5′-GACTACHVGGGTATCTAATCC-3′) and archaea (Arc349F: 5′-GYGCASCAGKCGMGAAW-3′/Arc806R: 5′- GGACTACVS GGGTATCTAAT-3′) (Takahashi et al., 2014). Sample-specific16-bp barcodes were incorporated into the primers for multiplex sequencing. The PCR components contained 5 μL of KAPA HiFi Buffer (5×), 0.75 μL of KAPA HiFi Hot Start DNA Polymerase (1U/μL), 0.75 μL (10 mM) of dNTPs, 0.75 μL (10 μM) of each Forward and Reverse primer, 2 μL of DNA Template, and 15 μL of ddH2O. Thermal cycling consisted of initial denaturation at 95°C for 5 s, followed by 25 cycles consisting of denaturation at 95°C for 30 s, annealing at 57°C for 30 s, and extension at 72°C for 60 s, with a final extension of 5 min at 72°C. PCR amplicons were purified with Agencourt AMPure Beads (Beckman Coulter, Indianapolis, IN) and quantified using the PicoGreen dsDNA Assay Kit (Invitrogen, Carlsbad, CA, USA). After the individual quantification step, PCR products were pooled in equal amounts. The pooled sample was then used to generate a library using SMRTbell Template Prep Kit 1.0-SPv3, and sequencing was conducted using an Illumina Miseq PE300 Sequencer system (Illumina Inc., San Diego, CA, USA).

2.4 Quality control, sequence assembly, and taxonomy assignment

Sequencing data were processed and analyzed using the software VSEARCH v2.7.0 and QIIME v1.9.1. The adapter and low-quality base pairs (bp) were identified and trimmed from the ends of the raw paired-end reads using Trim Galore v0.4.5, and then the short reads (< 100 bp) were removed. The paired-end reads were merged using VSEARCH, the sequences with low quality (total expected errors > 1) and shorter than 300 bp were discarded. The operational taxonomic units (OTUs) were clustered at 97% identity using the command cluster_fast (Rognes et al., 2016). Then, OTU-based chimera was detected using the command uchime_ref based on the Silva132 Database (Yilmaz et al., 2013). The taxonomy assignments for the representative sequence of the OTUs was conducted by BLAST against the Silva132 Database, using assign_taxonomy.py in QIIME (Caporaso et al., 2010). Taxonomy files and OTUs were further generated and the OTUs with less than 0.001% of total sequences in all samples were discarded. Before downstream analysis, 64,400 sequencing reads were obtained from the 5 samples after a flattening process. All raw data has been submitted to the NCBI Sequence Read Archive (accession code PRJNA973956).

2.5 Statistical analysis

All statistical analyses were performed using R software (version 4.1.1) with various packages. Alpha diversity indices (Shannon diversity, Simpson diversity, Chao1 richness, ACE richness) were used to assess the diversity of microbial communities, which were calculated using the "vegan" package (version 2.6-4) (Willis, 2019). Sparse curves were constructed using the "rarecurve" function ("vegan" package). Mantel's test ("LinkET" package, version 0.0.6.1) and Pearson's correlation analysis were performed to identify the subset of environmental variables that statistically explained the largest proportion of taxonomic unit variation (Legendre et al., 2015). Redundancy analysis (RDA, "vegan" package) was used to find environmental factors that could potentially explain community variances (Forester et al., 2018).

To visualize the analysis results, charts of geochemical parameters and mineral composition were plotted by Origin (version 2021). Microbial community compositions at the phylum level were illustrated as stacked bar charts by R ("ggplot2" package, version 3.4). The taxonomic abundance heatmap and Venn diagram were completed using the online tool Wekemo Bioincloud (https://www.bioincloud.tech). Chord diagrams were constructed using the online tool "circus" (http://circos.ca).

3 Results

3.1 Sampling sites and geochemical parameters

The three sampling sites (MS, CS, and FH) had distinct landscapes and habitats (Figure 1B). The MS site (stations ROV1 and ROV2) was an active seep with continuous methane bubbles. Live mussels and tubeworms were observed at this site. The FH site (stations ROV4 and ROV5) was a non-active seep without bubbles. Carbonate rocks, dead clams, and live king crabs were observed there. As the control, the CS site (station ROV3) was outside the active seep and had no characteristic faunal or rock.

Fundamental geochemical parameters, including TOC, IC, nitrate, sulfate, Mg, Ca, Sr, and median pore diameter, varied among the five sampling locations. Other parameters, including salinity, temperature, and dissolved oxygen, were relatively constant among these sites (Supplementary Table 1). The highest amounts of TOC and IC were found at the MS site. Peaks of 2.94% and 2.33% were observed for TOC and IC at ROV2 (Figure 2A). At the CS site, low values of 1.68% TOC and 1.57% IC were observed at ROV3. Notably, concentrations of sulfate and the metal elements Mg and Ca were highest at ROV2 (Figure 2B). Mg/Ca and Sr/Ca ratios were determined to identify the mineral type due to geochemical precipitation processes at these sites. The Mg/Ca ratios of all five sites were high, indicating that high-Mg calcite may be the dominant mineralogical composition of carbonate rocks at the Haima seep (Figure 2C). A maximum median pore diameter of 9.42 μm was observed at ROV2 (Figure 2C). The ROV2 site also had high organic matter and mineral content, which may be supporting numerous microorganisms and high chemosynthetic activity.

3.2 Microbial community structure and alpha diversity

The DNA of the microorganisms in the sampling sediment was extracted and sequenced. The average sequences of archaea and bacteria in samples from the five sites were 35,168 and 29,232 respectively. Rarefaction curves based on the archaeal and bacterial OTUs were plotted (Supplementary Figure 1). All of the curves reached an asymptote for the libraries of archaea and bacteria. Therefore, the sequencing data are sufficient to detect the presence of microbes and provide reliable results.

There was a difference in microbial community structure between the sites with and without methane-bubble seep. Site MS community was dominated by bacteria, accounting for 52–80% of the total sequences (Supplementary Figure 2). In contrast, archaea were more abundant at the FH site, contributing to 80–85% of the total populations. With respect to the archaeal community composition, Thaumarchaeota was the most abundant phylum in this area, especially at the sites of ROV1, ROV3, and ROV4 (Figure 3A). Notably, Euryarchaeota was the most abundant phylum ROV2 and ROV5. In terms of bacterial community composition, site ROV2 had a richer and more diverse set of taxa than the other sites (Figure 3B). *Proteobacteria* was the most abundant phylum at all sites except for ROV5 site, where Chloroflexi was the most abundant phylum. The relative

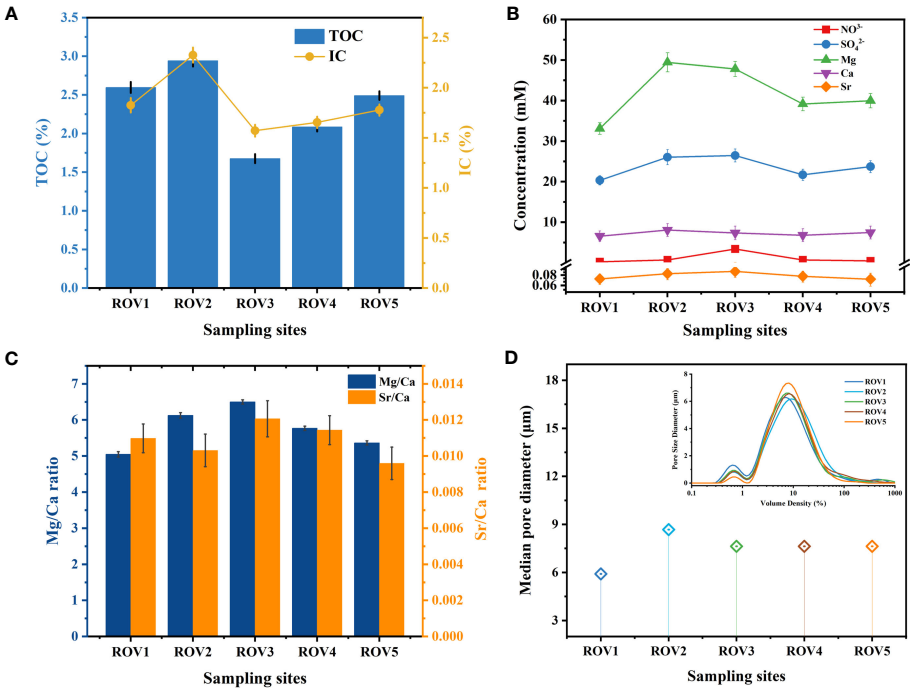

FIGURE 2
Fundamental geochemical parameters of sediments from the five sampling locations: organic content **(A)**, concentrations of the anions and metal elements **(B)**, Mg/Ca and Sr/Ca ratio **(C)**, and median pore diameter **(D)**.

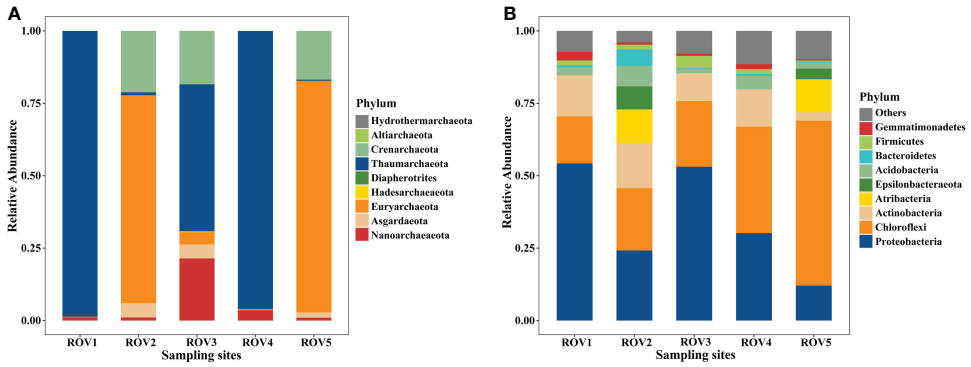

FIGURE 3
Relative abundance of phylum-level archaea **(A)** and bacteria **(B)** among the five sites.

abundance of archaeal and bacterial phyla varied among all five sites. The variability of community composition was visualized by Principal coordinate analysis (PCoA). The results showed that the distribution patterns of archaeal and bacterial genera at the MS and FH sites were similar, but the pattern at the CS site differed from other sites (Supplementary Figure 7). As shown in the genus heatmap (Figure 4), the distribution of top 25 abundant genera of bacteria was different between the MS site and FH site, but that of archaea was relatively similar between the two sites. Corresponding abundance relationships between all sites and the communities, including archaea and bacteria, were visualized using Circos analysis (Supplementary Figure 4). The relationships showed that site ROV2 had the least abundant archaeal genera and the most abundant bacterial genera. Notably, the genera associated with the SR-AOM process, such as *ANME-3*, *SEEP-SRB1*, and *SEEP-SRB4*, were found mainly distributed in site ROV2.

The fact that distinct habitats hosted quite different microbial communities (Figure 4) but shared many OTUs (Figure 5) means that compositional differences were generally a function of differential OTU relative abundance. The MS site exhibited approximately 40% lower archaeal OTU richness and 40% higher bacterial OTU richness than the other sites (Supplementary Figure 3). The analysis of OTU overlap among these sites revealed that microbial communities within the Haima seep area demonstrated clear differentiation according to habitat heterogeneity (Figure 5). The results indicated that microbial community shared only 88 (~9%) archaeal OTUs and 371 (~15%) bacterial OTUs across the habitats. The MS site had relatively less unique archaeal OTUs and more unique bacterial OTUs in comparison to the FH site. In terms of specific sites, the distribution of unique OTUs at each site is similar to the habitat to which it belongs. Therefore, both archaeal and bacterial communities were generally divided by habitat type, with significant differences among the distinct habitats of MS, FH, and CS sites within the Haima seep area.

We also explored the alpha diversity of archaeal and bacterial communities at sites with distinct habitats. Chao1 and ACE indices reveal community richness and estimate the number of OTUs in the samples (Kemp and Aller, 2004). The Chao1 and ACE indices of the MS site were different from those of both the CS and FH sites (Supplementary Figure 3). Archaeal richness was the lowest at site MS and the highest at site FH, whereas the bacterial richness was the highest at site MS and lowest at site FH. Shannon and Simpson indices are used to describe community diversity (Chao et al., 2014). The Shannon and Simpson indices of the CS site were different from those of both the MS and FH sites (Supplementary Figure 3). Community diversity was low when the Shannon index was small and the Simpson index was large. As a result, the bacterial diversity at the CS site and the archaeal diversities at the MS and FH sites were low.

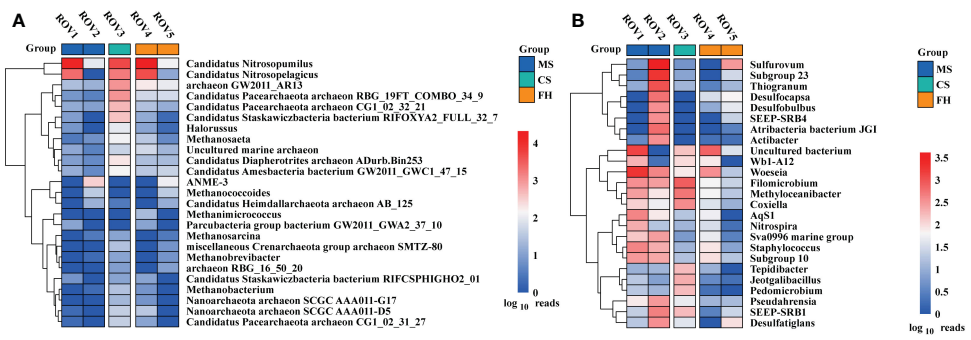

FIGURE 4
Heatmaps based on the 25 most abundant genera of archaea **(A)** and bacteria **(B)** at the five sites.

10.3389/fmars.2023.1254450

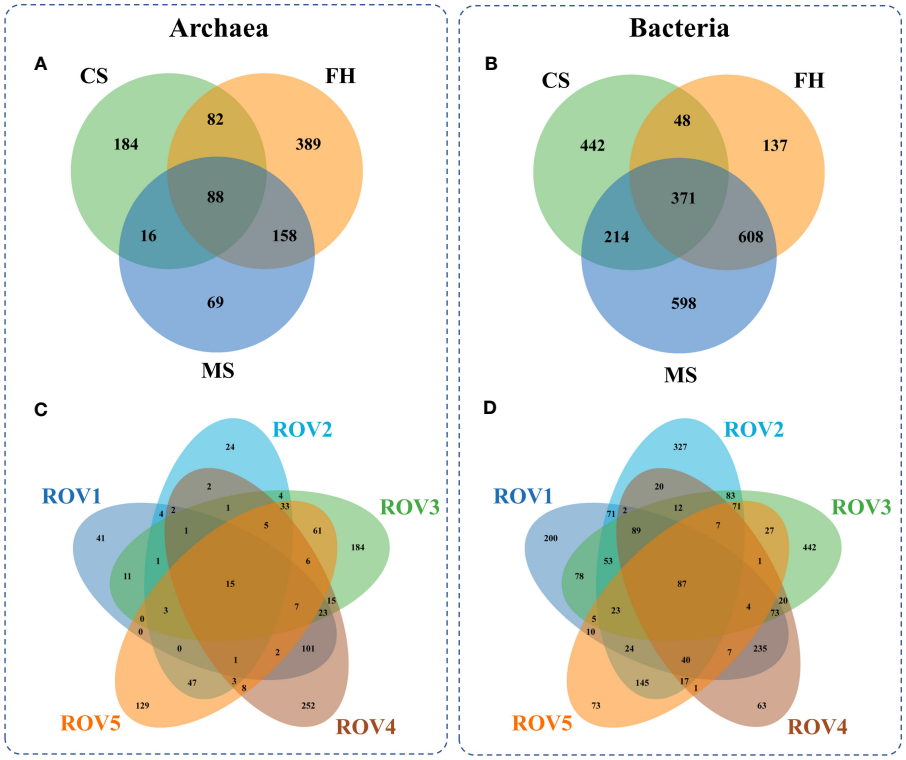

FIGURE 5
Archaeal OTU overlap among various habitats **(A)** and sampling sites **(C)**, and bacterial OTU overlap among the habitats **(B)** and the sites **(D)**.

3.3 Correlations among microbial community structure, mineral assemblages, and environmental factors

To explore the key environmental variables and mineral assemblages that may have shaped microbial community composition, correlations between the microbial diversity and the variables were evaluated using RDA analysis and a permutation test based on the relative abundance at the genus level. Quantification of major environmental and mineral parameters, including TOC, IC, NO_3^-, SO_4^{2-}, Ca, Mg, Na, Sr, D50, Illite, Clinochlore, Quartz, Albite, Calcite, and Halite, was used for RDA analysis. The permutation test indicated that TOC made a statistically significant ($p < 0.05$) contribution to explaining the variance in archaeal communities (Figure 6A). Comparatively, Ca, SO_4^{2-}, Mg, and calcite were suggested as the most significant ($p < 0.01$) environmental factors in the bacterial communities (Figure 6B). Notably, site ROV2 was most relevant to the key variables of TOC, IC, Ca, and calcite, indicating that this site may have a strong correlation with the process of carbonate precipitation. In addition, characteristic genera

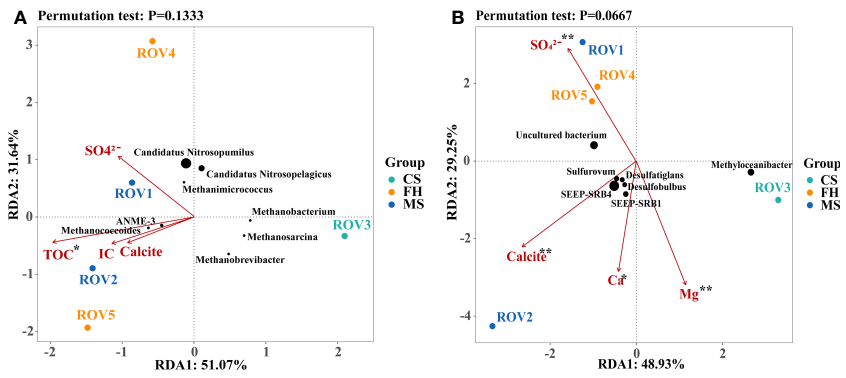

FIGURE 6
Redundancy analysis (RDA) correlation of the environmental and mineral variables to archaeal **(A)** and bacterial **(B)** communities. The green, yellow, and blue dots in the figure represent the sites CS, FH, and MS, respectively. The black points indicate the characteristic genera, and their sizes represent the genera abundance. The pink arrows indicated individual environmental and mineral parameters. Significance levels (marked by asterisks) were based on the permutation test. **$p < 0.01$; *$p < 0.05$.

such as *ANME-3*, *SEEP-SRB1*, and *SEEP-SRB4* showed a strong correlation with the key variables of carbonate precipitation.

Environmental drivers at the habitats in the Haima seep were identified based on our dataset to validate the independence of the microbial communities at different habitats. Differences in bacterial and archaeal community composition were correlated with differences in environmental factors as shown in Figure 7. The results showed that SO_4^{2-}, Mg, and calcite were the strongest correlates (<0.01) with bacterial community composition in the habitats. In addition, IC, Ca, and calcite were found to be significantly correlated (<0.05) with bacterial community composition. Thus, the environmental drivers of microbial communities in the habitats in the Haima area are mainly SO_4^{2-}, Ca, Mg, and Calcite, all of which are associated with mineralization processes.

3.4 Mineral assemblages in cold seep habitats

Minerals from sediment at the five Haima area sampling sites showed a relatively similar composition (Figure 8). The minerals in the sediments included illite, clinochlore, quartz, albite, calcite, and halite (Figure 8A). The results indicate that most of the sediments in Haima seep were dominated by siliciclastic minerals such as quartz and illite. Quartz content varied between 19% and 38%, and illite content ranged from 16% to 31% (Figure 8B). Sample ROV2 was dominated by calcite (48%), which was the major microcrystalline carbonate phase. Due to the ROV2 site was in a methane-seep habitat and had abundant genera associated with the SR-AOM process (Figure 4), the mineralization of authigenic carbonate at this site may relate to the methane-seep process. The calcite content varied between 2% and 12% at the other sites. In the FH site, Sample ROV5 had a relatively high amount (~12%) of authigenic carbonate.

Minerals with distinct morphologies from different habitats of the Haima area were observed using SEM (Figure 9). The mineral samples were observed to be mostly clastic mineral forms 10 μm in size. High levels of terrestrial clasts were found in the sites of ROV1, ROV3, and ROV4 (Figures 9A, C, D). The mineral phases at these sites were dominated by illite and quartz, while authigenic calcite was rarely present (Figure 8B). By contrast, authigenic calcite had a relatively high distribution at site ROV2 (Figure 9B) and was locally present at site ROV5 (Figure 9E). This phenomenon was related to the relatively high content of Ca and organic carbon at sites ROV2 and ROV5 and the abundance of methane cycle taxa (Figures 2, 3). Interestingly, some calcite showed axial growth morphology (Figures 9B, E), suggesting that it may have formed from authigenic carbonates. In addition, carbonates were present in different mineral forms. Carbonate minerals at site ROV2 exhibited not only strip morphology but also flake and block morphology (Supplementary Figure 5).

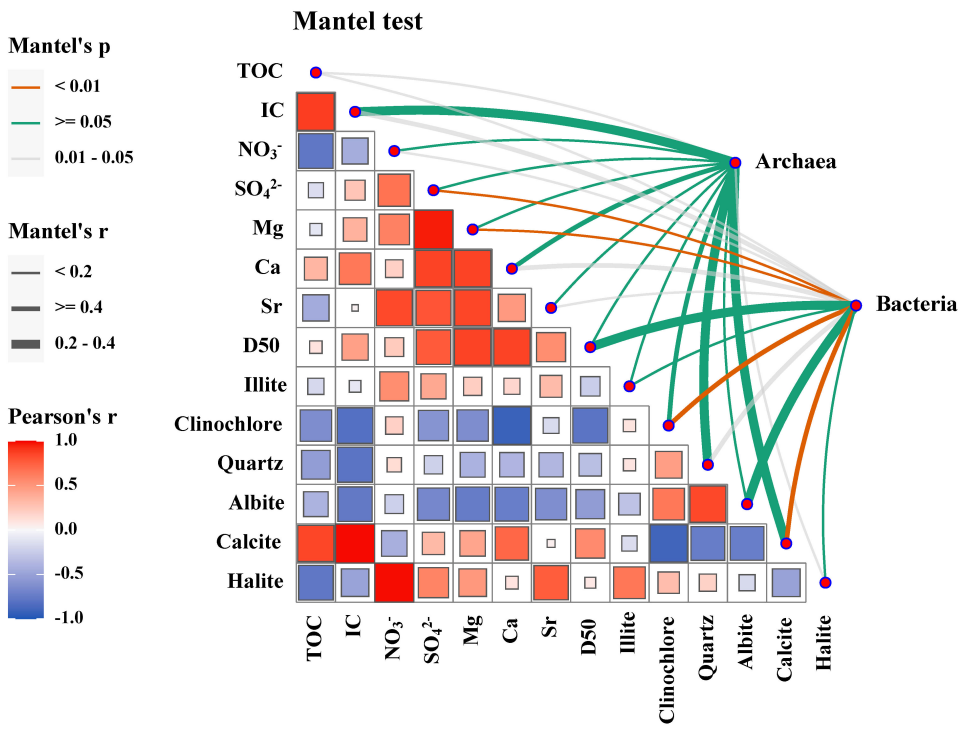

FIGURE 7
Environmental drivers of the microbial community compositions. Pairwise comparisons of environmental and mineral variables are shown, with a color gradient indicating Spearman's correlation coefficients. The community composition of genera was related to each variable by partial Mantel tests. Edge width corresponds to the Mantel's r statistic for the corresponding distance correlations, and edge color denotes the statistical significance based on the permutation test.

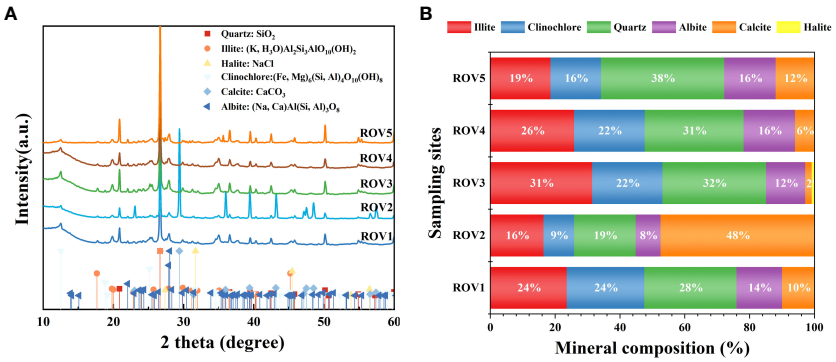

FIGURE 8
XRD patterns **(A)** of minerals in cold-seep habitats. Mineral composition **(B)** of the sediment sample was characterized by illite, clinochlore, quartz, albite, calcite, and halite.

3.5 Indicator microbes associated with SR-AOM and mineralization in different habitats

Calcite-dominated minerals were identified at site ROV2 (Figure 8B). They were mainly authigenic carbonates resulting from biological mineralization (Li et al., 2018a). SR-AOM is considered an organic matter mineralization process (Han et al., 2013). The distribution of indicator microbes associated with this process at each sample site was evaluated (Figure 10). The results indicate that the taxa associated with SR-AOM processes were found in relatively low relative abundance (<10%) at sites ROV1, ROV3, and ROV4, while significant enrichment of *ANME-3*, *Methanococoides*, *Sulfurovum*, *Desulfocapsa*, and *SEEP-SRB2* was identified at sites ROV2 and ROV5. The dominant genus *ANME-3*, which induces the AOM process, had a relative abundance in

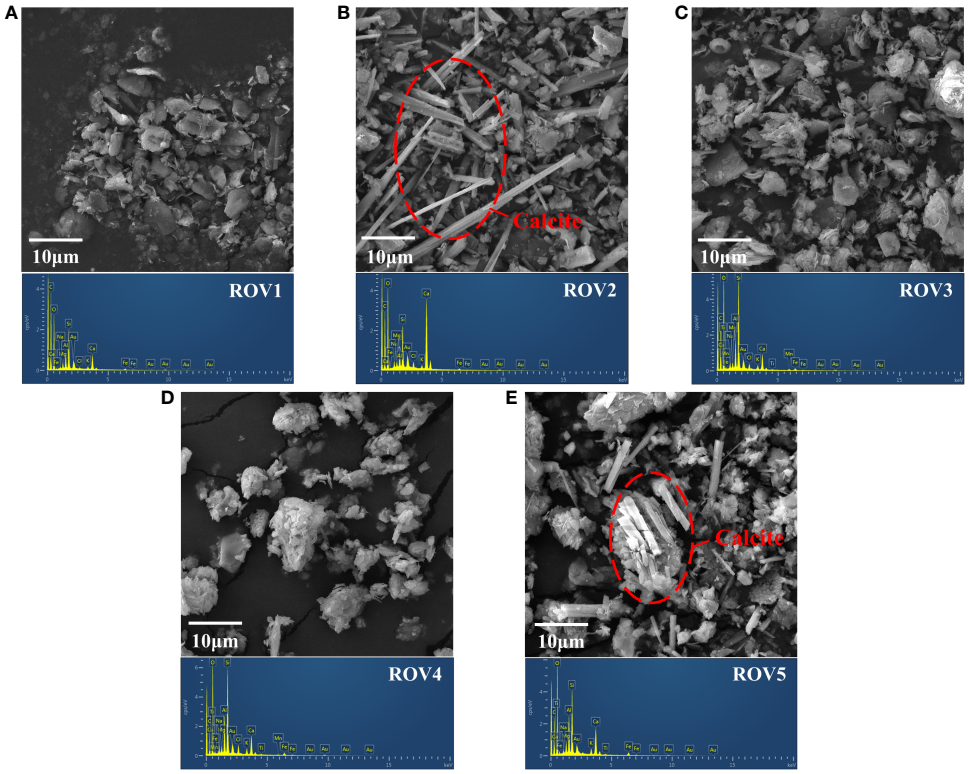

FIGURE 9
Multiple morphologies of minerals in various habitats at the Haima seep. The SEM images of minerals at the sites ROV1 **(A)**, ROV2 **(B)**, ROV3 **(C)**, ROV4 **(D)**, and ROV5 **(E)**. Calcite is marked by a red arrow.

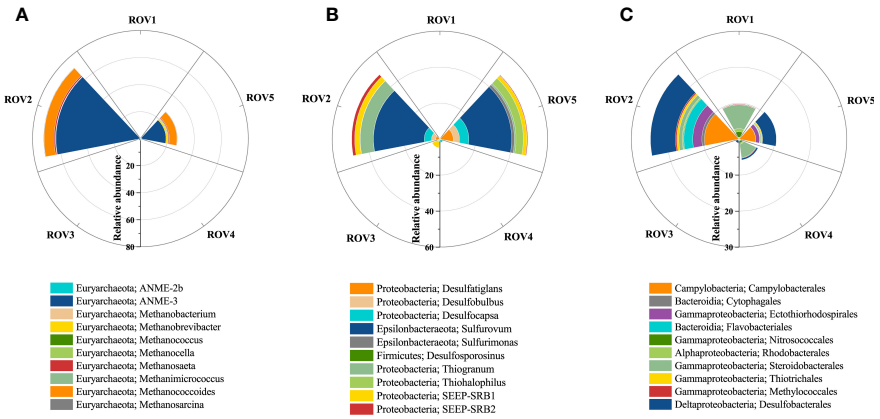

FIGURE 10
Signature microbes associated with the processes of SR-AOM and mineralization. Relative abundance of AOM-related genera **(A)**, SR-related genera **(B)**, and mineralization-related microbes at order level **(C)** in the seep area.

archaea of 62.3% in ROV2 and 18.1% in ROV5 (Figure 10A). The genus *Sulfurovum*, which induces the SR process, had a relative abundance in bacteria of 28.3% at ROV2 and 23.8% at ROV5 (Figure 10B). These organisms were likely supported by the high organic carbon content and sulfate concentration in the seep areas (Figure 2). Euryarchaeota *ANME-3* and Epsilonbacteraeota *Sulfurovum* were found to be characteristic of microorganisms in seep sediments of the Haima area (Niu et al., 2017). Our data corroborate this finding.

Taxa related to authigenic carbonates, such as Campylobacterales, Desulfobacterales, and Ectothiorhodospirales, were found to be present in the Haima area (Figure 10C). The taxa composition was similar to carbonate-host microbes that are considered early successional communities of carbonate biofilms (Case et al., 2015; Leprich et al., 2021). The abundance of those taxa was relatively high at sites ROV2 and ROV5 and was significantly different from that at other sites. Therefore, minerals with high carbonate content were associated with the enriched indicator microbes. Correlations of mineral and environmental factors with the abundance of indicator microbes were analyzed (Supplementary Figure 6). The results show that the abundance of Desulfobacterales was strongly correlated ($p < 0.001$) with Ca concentration variation, and the abundance of Campylobacterales, Thiotrichales, and Ectothiorhodospirales was significantly correlated with calcite content ($p < 0.05$). In addition, the abundance of genera such as *ANME-3*, *Methanococoides*, and *SEEP-SRB2* was significantly correlated ($p < 0.05$) with changes in Ca concentration and calcite content (Supplementary Figures 6A, B), suggesting that the SR-AOM process was strongly associated with the process of carbonate formation.

4 Discussion

We conducted this comprehensive study of the variability in microbial communities, environmental factors, and mineral assemblages among different habitats to explore how microbial communities and mineral assemblages were shaped by the distinct habitats in the Haima seep area. Surface sediments were collected from different habitats including methane seep sites, seep-free faunal habitats, and a seep-free control site in the Haima area. Different microbial communities and mineral compositions revealed environmental controls on the relative importance of the biogeochemical processes. Environmental factors were likely to influence microbial community structure and thus authigenic mineral formation. These observations invoke questions about the linkage between environmental factors, microbial communities, and mineral assemblages in the sediments of Haima.

4.1 Geochemical characteristics of different habitats in the Haima seep

Characteristics of sediment from the Haima area revealed that environmental factors varied among habitats. The amount of organic matter and metal ions was higher in the seep habitat compared with other habitats. Organic carbon and metal elements in subsurface sediments were possibly sourced from deep fluids associated with methane seepage (Pierre et al., 2017). The TOC and IC were highest at site ROV2 (Figure 2A), indicating that microbially induced carbon cycling was active at this site (Dan et al., 2023). The high content of TOC indicated methane seepages, abundant microorganisms, and organic metabolites (Valentine et al., 2005). High IC suggests the presence of organic matter mineralization at the site (Núñez-Useche et al., 2018). Intense AOM promotes the combination of oversaturated HCO_3^- with metal ions and leads to the precipitation of carbonate minerals (Baker and Burns, 1985). TOC and IC were higher at the Haima sampling sites than at other cold seep areas in the SCS (Li et al., 2018b; Zhuang et al., 2019; Zhang et al., 2022b). TOC and IC can indicate the geochemical processes of methane seepage activity, as explained in recent studies on the long history of cold seep evolution in the Haima (Zhang et al., 2022a; Dan et al., 2023).

Sulfate acts as an important electron acceptor for the AOM process, and variations in its concentration affect the efficiency of

SR-AOM (Boetius et al., 2000). The levels of sulfate at the sampling sites were consistent with Haima seep sediments from previous studies (Zhuang et al., 2019; Liu et al., 2020; Huang et al., 2023). At ROV2 and ROV5, the sulfate concentrations in the sediments were relatively high (Figure 2B), implying a potentially high geochemical reactivity, especially SR-AOM (Li et al., 2020). Sulfate concentration was controlled by the upper water column, and the difference in its distribution affected the reaction efficiency of AOM (Orcutt et al., 2005). Since authigenic carbonate was one of the products of the AOM process, its content can be indirectly affected by sulfate (Li et al., 2018a). In addition, the relatively large grain size of sediments at ROV2 indicated the presence of numerous large-grained minerals (Figure 2D). The minerals were mostly authigenic carbonates (Figure 8B), which usually precipitate at seep sites due to the AOM reaction and gradually form carbonate rocks (Caesar et al., 2019).

To evaluate the potential of biological mineralization in the study area, we investigated the substances associated with authigenic carbonates. Variations in Ca^{2+}, Mg^{2+}, and Sr^{2+} concentrations can be used to identify the mineral phases of carbonate precipitation (Nöthen and Kasten, 2011; Liu et al., 2020). In this study, the metal elements Mg and Ca were at high levels at ROV2 (Figure 2B). The Mg/Ca ratio was also relatively high (Figure 2C). The results indicate that authigenic carbonate precipitation may have occurred in the sediments. The mineral composition of carbonates in cold seeps can be used to indicate seepage intensity (Roberts et al., 2010; Nöthen and Kasten, 2011). Carbonates were the most abundant minerals at site ROV2 (Figure 8), suggesting a high-activity methane seepage at this location. XRD analysis results of carbonate minerals are consistent with findings in other reports that calcite is one of the authigenic carbonate minerals formed in the cold seep system (Naehr et al., 2007; Liu et al., 2020). Calcite has been proven to preferentially precipitate in sediments with low sulfate concentrations due to the inhibition of calcite precipitation by sulfate ions (Nöthen and Kasten, 2011; Hu et al., 2015). In this study, the sulfate concentrations at the sampling sites were at high levels (>20 mM, Figure 2B), which may be an important reason for the generally low calcite content in the area (except at site ROV2). In addition, the Sr/Ca of aragonite is higher than that of seawater, and thus the precipitation of aragonite will lead to lower Sr/Ca in pore water (Nöthen and Kasten, 2011). The Sr/Ca ratio at ROV2 was low (Figure 2C), so it was inferred that a very small amount of aragonite precipitation may be present at this site. Therefore, we suggest that environmental factors such as Mg, Ca, and SO_4^{2-} concentrations were important factors influencing the formation of authigenic carbonate minerals.

4.2 Microbial community similarity and variability among different habitats

Similarities and variability of archaeal and bacterial communities were found in different habitats of the seep area. Dominant archaeal groups, such as Thaumarchaeota and Euryarchaeota, were consistently detected at all five sites (Figure 3A). These archaea are widespread in marine seep sediments (Cui et al., 2019; Jing et al., 2020; Xin et al., 2022), and they largely constrain the ecological roles in local habitats. Thaumarchaeota, an aerobic archaeal phylum capable of ammonium oxidation, can be involved in various biogeochemical processes, including but not limited to nitrification and carbon fixation (Offre et al., 2013). Some of its members are chemoorganotrophs with multiple functions such as aerobic mineralization of organic matter (Adam et al., 2017). The archaea at ROV2 had the lowest abundance compared with other sites (Supplementary Figure 2), and were simple in composition, with the dominant phylum being Euryarchaeota (relative abundance >70%, Figure 3A). The taxa of Euryarchaeota, such as methanogens and methanotrophs, are mostly associated with methane cycling processes consisting of methane production and the anaerobic oxidation of methane (Jing et al., 2020; Fischer et al., 2021). A previous study has indicated that methane oxidation and methane production occur simultaneously in seep sediments although the AOM process dominates at the site (Orcutt et al., 2005). In this study, enriched *Methanococcoides* and *ANME-3* were detected simultaneously at the seep site (Figure 10A). Thus, our results support the notion that methane-seep habitats have high relative proportions of methane-cycling communities.

For bacterial communities in our study, Proteobacteria and Chloroflexi were dominant at the sampling sites (Figure 3B). Phylum Chloroflexi is widely distributed and diverse in the marine environment, but poorly characterized (Zhang et al., 2012). Chloroflexi generally dominates pelagic or organic-rich seafloor sediments (Inagaki et al., 2003). The large number of benthic fauna found at ROV4 and ROV5 supports this finding (Figure 1B). Proteobacteria are found in high relative abundance and phylogenetic diversity in various marine habitats (Cui et al., 2019; Xin et al., 2022). Heterotrophic Proteobacteria are deeply involved in the sulfur cycle through the sulfate reduction mediated by *SEEP-SRB1* and the sulfur oxidation mediated by *Sulfurovum*. SR-related genera associated with particular ANME partners contribute to carbon cycling through the SR-AOM process (Chen et al., 2022b).

In this study, the diversity and relative abundance of archaea were low at the MS site, while bacteria were high (Supplementary Figure 3). The abundance of unique archaeal OTUs was lowest in the methane-seep habitat compared with the other habitats (Figure 5). Comparatively, the abundance of unique bacterial OTUs was highest in the methane-seep habitat compared with the other habitats. This spatial distribution is consistent with other studies (Niu et al., 2017; Xin et al., 2022) and is caused by the heterogeneity of the geochemistry of different habitats. The MS site and the seep-free FH site shared more archaea and bacteria OTUs than any other two habitats, indicating an overall similarity between them (Figure 5; Supplementary Figure 7). Methane-seep habitat and faunal habitat belong to different developmental stages of cold seeps (Feng et al., 2023). The microbial communities in the faunal habitat are largely sourced from the cold seep vent, and they are symbiotic with seep fauna such as mussels and clams (Chen et al., 2022b). The fauna is supplied with metabolic material and energy by the chemoautotrophic microbes. In both habitats, although ROV2

and ROV5 sites showed similarities, whereas ROV2 had more AOM- and SR-related genera and produced more authigenic carbonates compared to ROV5 (Figures 8, 10). Thus, the SR-AOM process differs in reactivity across distinct habitats within a cold seep area. Further, habitat heterogeneity contributes to differences in methane oxidation efficiency, thereby influencing carbon cycling in cold seeps.

Community distribution in cold seep areas is closely related to the location of the seepage. The microbial taxa associated with SR-AOM reflect different levels of activity at different sites (Zhuang et al., 2019). In this study, ANME was detected at ROV2 (Figure 4A), indicating high methane oxidation activity at this site. *ANME-2* was the most widespread and abundant clade, yet only a small amount of *ANME-2b* (<5%) was detected at the Haima seep site (Figure 10A). In contrast to previous investigations, *ANME-3* is detected as the dominant clade of the methane-metabolizing genus (relative abundance >60%, Figure 10A). *ANME-3* was generally found in mud volcanoes and some seep sediments (Niemann et al., 2006). Thus, it was reasonable for *ANME-3* to be present in seep sediment at our sampling sites. On the other hand, sulfate-cycling bacteria were highly diverse and varied widely between sites. They were dominated by *Sulfurovum* at ROV2 and ROV5, while relatively high abundances of *SEEP-SRB1*, *SEEP-SRB2*, and *SEEP-SRB4* were also present (Figure 10B). This is consistent with a previous report that *Sulfurovum* is abundant in the surface sediments of a cold seep (Li et al., 2021). *Sulfurovum*, the sulfur-oxidizing member of Epsilonbacteraeota, uses CO_2 produced by ANME as a carbon source and is able to oxidize sulfide produced by SRB to sulfate (Liu et al., 2016). *Sulfurovum* is involved in carbon fixation and sulfur oxidation in marine ecosystems. Through the sulfur oxidation, sulfur bioavailability is further enhanced to support the metabolism of SRB, thereby facilitating the SR-AOM process. Thus, functionally diverse sulfur-cycling bacteria coupled with methane oxidation support carbon cycling in cold seep habitats.

4.3 Linkage between environmental factors, microbial community, and mineral assemblage

The effect of habitat heterogeneity on community diversity and mineral assemblage was evident. We found that the diversity of microbial communities in habitats was affected by environmental factors. The variables with statistical differences between habitats were SO_4^{2-}, Ca, Mg, and TOC (Figures 6, 7). SO_4^{2-} has been proven to be the most important factor in the structure of the microbial bacterial community in the sediment environment (Orcutt et al., 2005; Zhuang et al., 2019). Sulfate is abundant at the seep and SR is the main terminal electron-accepting process. The availability of the electron acceptor SO_4^{2-} may drive the distribution of methane oxidizers (Li et al., 2020). In addition, the distribution of the archaeal community may be influenced by high organic carbon in the habitat. The high organic carbon represented abundant organic matter or methane, indicating that both methanogens and methanotrophs may be present in this habitat (Jing et al., 2020; Fischer et al., 2021). Therefore, different environmental conditions are selected for different types of methane metabolizing communities.

Authigenic carbonate precipitation induced by AOM is an important sink in marine carbon cycling (Marlow et al., 2014; Marlow et al., 2021). Our results showed that the IC content and the concentrations of alkaline earth elements (Mg, Ca, and Sr) were relatively high at ROV2 (Figure 2), indicating that authigenic carbonate precipitation occurred in the sediments (Figure 9). Different carbonate mineralogy was inferred through the relationship between Sr/Ca and Mg/Ca ratios in the pore water (Nöthen and Kasten, 2011; Liu et al., 2020). The high Mg/Ca ratios (>5) in pore water indicated the occurrence of possible primary high-Mg calcite (Bayon et al., 2007). The precipitation of high-Mg calcite may indicate a relatively low-activity seep environment (Hu et al., 2015). *ANME-3* found in association with the *Desulfobulbus* has been determined to oxidize seafloor methane and deliver reductants to their synthetic partner (Niemann et al., 2006). AOM produces two units of alkalinity per one unit of dissolved inorganic carbon, increasing the alkalinity of the pore water and promoting the precipitation of authigenic carbonate minerals (Aloisi et al., 2002).

The formation of carbonate minerals not only occurs through biological mineralization of organic matter but also is facilitated by the secretion of extracellular macromolecules by specific microbes (Wei et al., 2021). In this study, strong correlations with carbonate were found for Campylobacterales and Desulfobacterales (Supplementary Figure 6). These taxa are considered early successional communities of carbonate biofilms (Case et al., 2015; Leprich et al., 2021; Marlow et al., 2021). Campylobacterales attach to mineral surfaces and dominate the formation of biofilm communities. Desulfobacterales, as heterotrophic bacteria, are believed to have a potential role in the production of the extracellular matrix. The amounts of exopolymeric substances can affect the morphology and mineralogy of the carbonate minerals (Braissant et al., 2007). Interactions between elemental Ca and exopolymeric substances are the main processes by which the extracellular matrix controls the precipitation of carbonate minerals.

In general, the environmental characteristics of the habitat and the benthic microorganisms collectively influenced the mineral assemblages. Environmental drivers such as SO_4^{2-}, Ca, and Mg shaped the microbial communities in seep habitats. The SR-AOM and mineralization processes induced by microbes were affected by the seepage activity in the habitat. Microbial metabolism altered the environmental factors, leading to changes in the precipitation conditions of certain minerals. Thus, the formation of authigenic carbonate minerals resulted in variations of mineral assemblages in different habitats.

5 Conclusion

We conducted a comprehensive biogeochemical and mineralogical study to investigate microbial community structure, mineral assemblages, and their relationship with environmental variations in different habitats in the Haima seep, SCS. Archaeal and bacterial composition and abundance were significantly different in the three habitats (MS, FH, and CS). By contrast, the archaeal composition in sites ROV2 and ROV5 was similar. The most abundant SR-AOM and mineralization process-related taxa

occurred at site ROV2, indicating the highest seepage activity and most active mineralization at that location. A high amount of calcite minerals was found at the seep, suggesting that the high activity of SR-AOM was accompanied by the formation of authigenic carbonate minerals. Significant correlations between bacterial communities, calcite, and environmental factors such as SO_4^{2-}, Ca, and Mg revealed that the formation of authigenic carbonate was an important process influencing the mineral assemblages in seep habitats. Our study illustrated the geochemical, microbiological, and mineralogical characteristics of cold seep habitats in the Haima area and improved our understanding of microbe-induced carbon cycling and the formation of authigenic carbonate.

Data availability statement

The datasets presented in this study can be found in the online repository. The names of the repository and accession number can be found below: NCBI Sequence Read Archive (accession code PRJNA973956).

Author contributions

JL: Formal Analysis, Methodology, Writing – original draft, Writing – review & editing. JF: Conceptualization, Funding acquisition, Supervision, Writing – review & editing. JK: Data curation, Writing – review & editing. YH: Data curation, Writing – review & editing. HZ: Methodology, Writing – review & editing. SongZ: Methodology, Writing – review & editing. LT: Software, Visualization, Writing – review & editing. SiZ: Supervision, Writing – review & editing.

Funding

The author(s) declare financial support was received for the research, authorship, and/or publication of this article. We acknowledge the financial support for this research that was received from the National Key Research and Development Program (2021YFF0502300), the National Natural Science Foundation of China (42325603, 41890850, 42022046, and 42227803), Guangdong Natural Resources Foundation (GDNRC [2022]45), PI project of Southern Marine Science and Engineering Guangdong Laboratory (Guangzhou) (GML20190609, GML2022009, GML20230921), and Guangdong Provincial Key Laboratory Project (2019B121203011).

Acknowledgments

We are grateful to the crew of the RV Haiyang-6 and ROV Haima team for their assistance in collecting the samples.

Conflict of interest

The authors declare that the research was conducted in the absence of any commercial or financial relationships that could be construed as a potential conflict of interest.

Publisher's note

Supplementary material

The Supplementary Material for this article can be found online at: https://www.frontiersin.org/articles/10.3389/fmars.2023.1254450/full#supplementary-material

References

Adam, P. S., Borrel, G., Brochier-Armanet, C., and Gribaldo, S. (2017). The growing tree of Archaea: new perspectives on their diversity, evolution and ecology. *ISME J.* 11 (11), 2407–2425. doi: 10.1038/ismej.2017.122

Aloisi, G., Bouloubassi, I., Heijs, S. K., Pancost, R. D., Pierre, C., Sinninghe Damsté, J. S., et al. (2002). CH4-consuming microorganisms and the formation of carbonate crusts at cold seeps. *Earth Planetary Sci. Lett.* 203 (1), 195–203. doi: 10.1016/S0012-821X(02)00878-6

Baker, P. A., and Burns, S. J. (1985). Occurrence and formation of dolomite in organic-rich continental margin sediments. *Bulletin Am. Assoc. Petroleum Geologists* 69 (11), 1917–1930. doi: 10.1306/94885570-1704-11D7-8645000102C1865D

Bayon, G., Pierre, C., Etoubleau, J., Voisset, M., Cauquil, E., Marsset, T., et al. (2007). Sr/Ca and Mg/Ca ratios in Niger Delta sediments: Implications for authigenic carbonate genesis in cold seep environments. *Mar. Geology* 241 (1), 93–109. doi: 10.1016/j.margeo.2007.03.007

Boetius, A., Ravenschlag, K., Schubert, C. J., Rickert, D., Widdel, F., Gieseke, A., et al. (2000). A marine microbial consortium apparently mediating anaerobic oxidation of methane. *Nature* 407 (6804), 623–626. doi: 10.1038/35036572

Bowles, M., Hunter, K. S., Samarkin, V., and Joye, S. (2016). Patterns and variability in geochemical signatures and microbial activity within and between diverse cold seep habitats along the lower continental slope, Northern Gulf of Mexico. *Deep-Sea Res. Part Ii-Topical Stud. Oceanography* 129, 31–40. doi: 10.1016/j.dsr2.2016.02.011

Braissant, O., Decho, A. W., Dupraz, C., Glunk, C., Przekop, K. M., and Visscher, P. T. (2007). Exopolymeric substances of sulfate-reducing bacteria: Interactions with calcium at alkaline pH and implication for formation of carbonate minerals. *Geobiology* 5 (4), 401–411. doi: 10.1111/j.1472-4669.2007.00117.x

Caesar, K. H., Kyle, J. R., Lyons, T. W., Tripati, A., and Loyd, S. J. (2019). Carbonate formation in salt dome cap rocks by microbial anaerobic oxidation of methane. *Nat. Commun.* 10 (1), 808. doi: 10.1038/s41467-019-08687-z

Cao, L., Lian, C., Zhang, X., Zhang, H., Wang, H., Zhou, L., et al. (2021). *In situ* detection of the fine scale heterogeneity of active cold seep environment of the Formosa Ridge, the South China Sea. *J. Mar. Syst.* 218, 103530. doi: 10.1016/j.jmarsys.2021.103530

Caporaso, J. G., Kuczynski, J., Stombaugh, J., Bittinger, K., Bushman, F. D., Costello, E. K., et al. (2010). QIIME allows analysis of high-throughput community sequencing data. *Nat. Methods* 7 (5), 335–336. doi: 10.1038/nmeth.f.303

Case, D. H., Pasulka, A. L., Marlow, J. J., Grupe, B. M., Levin, L. A., and Orphan, V. J. (2015). Methane seep carbonates host distinct, diverse, and dynamic microbial assemblages. *mBio* 6 (6), e01348–e01315. doi: 10.1128/mBio.01348-15

Chao, A., Gotelli, N. J., Hsieh, T. C., Sander, E. L., Ma, K. H., Colwell, R. K., et al. (2014). Rarefaction and extrapolation with Hill numbers: a framework for sampling and estimation in species diversity studies. *Ecol. Monogr.* 84 (1), 45–67. doi: 10.1890/13-0133.1

Chen, C., Zhong, L., Wan, Z., Cheng, C., Zhou, W., and Xu, X. (2022a). Geochemical characteristics of cold-seep carbonates in Shenhu area, South China Sea. *J. Oceanology Limnology* 40 (3), 969–985. doi: 10.1007/s00343-021-1112-z

Chen, Y., Lyu, Y., Zhang, J., Li, Q., Lyu, L., Zhou, Y., et al. (2022b). Riddles of lost city: chemotrophic prokaryotes drives carbon, sulfur, and nitrogen cycling at an extinct cold seep, South China sea. *Microbiol. Spectr.* 0 (0), e03338–e03322. doi: 10.1128/spectrum.03338-22

Cui, H., Su, X., Chen, F., Holland, M., Yang, S., Liang, J., et al. (2019). Microbial diversity of two cold seep systems in gas hydrate-bearing sediments in the South China Sea. *Mar. Environ. Res.* 144, 230–239. doi: 10.1016/j.marenvres.2019.01.009

Dan, X., Liu, S., Feng, X., Lin, L., Tang, R., Yang, C., et al. (2023). Geochemical record of methane seepage in carbon cycling and possible correlation with climate events in the Qiongdongnan basin, South China Sea. *Mar. Petroleum Geology* 149, 106061. doi: 10.1016/j.marpetgeo.2022.106061

Feng, J.-C., Li, C.-R., Tang, L., Wu, X.-N., Wang, Y., Yang, Z., et al. (2023). Tracing the century-long evolution of microplastics deposition in a cold seep. *Advanced Sci.* 10, 2206120. doi: 10.1002/advs.202206120

Feng, J.-C., Liang, J., Cai, Y., Zhang, S., Xue, J., and Yang, Z. (2022a). Deep-sea organisms research oriented by deep-sea technologies development. *Sci. Bull.* 67 (17), 1802–1816. doi: 10.1016/j.scib.2022.07.016

Feng, J.-C., Yan, J., Wang, Y., Yang, Z., Zhang, S., Liang, S., et al. (2022b). Methane mitigation: Learning from the natural marine environment. *Innovation* 3 (5), 100297. doi: 10.1016/j.xinn.2022.100297

Feng, J.-C., Yang, Z., Zhou, W., Feng, X., Wei, F., Li, B., et al. (2022c). Interactions of microplastics and methane seepage in the deep-sea environment. *Engineering*. 8(9). doi: 10.1016/j.eng.2022.08.009

Fischer, P. Q., Sánchez-Andrea, I., Stams, A. J. M., Villanueva, L., and Sousa, D. Z. (2021). Anaerobic microbial methanol conversion in marine sediments. *Environ. Microbiol.* 23 (3), 1348–1362. doi: 10.1111/1462-2920.15434

Forester, B. R., Lasky, J. R., Wagner, H. H., and Urban, D. L. (2018). Comparing methods for detecting multilocus adaptation with multivariate genotype-environment associations. *Mol. Ecol.* 27 (9), 2215–2233. doi: 10.1111/mec.14584

Guan, H., Birgel, D., Peckmann, J., Liang, Q., Feng, D., Yang, S., et al. (2018). Lipid biomarker patterns of authigenic carbonates reveal fluid composition and seepage intensity at Haima cold seeps, South China Sea. *J. Asian Earth Sci.* 168, 163–172. doi: 10.1016/j.jseaes.2018.04.035

Han, X. Q., Yang, K. H., and Huang, Y. Y. (2013). Origin and nature of cold seep in northeastern Dongsha area, South China Sea: Evidence from chimney-like seep carbonates. *Chin. Sci. Bull.* 58 (30), 3689–3697. doi: 10.1007/s11434-013-5819-x

Hu, Y., Feng, D., Liang, Q., Xia, Z., Chen, L., and Chen, D. (2015). Impact of anaerobic oxidation of methane on the geochemical cycle of redox-sensitive elements at cold-seep sites of the northern South China Sea. *Deep Sea Res. Part II: Topical Stud. Oceanography* 122, 84–94. doi: 10.1016/j.dsr2.2015.06.012

Huang, Y., Feng, J.-C., Kong, J., Sun, L., Zhang, M., Huang, Y., et al. (2023). Community assemblages and species coexistence of prokaryotes controlled by local environmental heterogeneity in a cold seep water column. *Sci. Total Environ.* 868, 161725. doi: 10.1016/j.scitotenv.2023.161725

Inagaki, F., Suzuki, M., Takai, K., Oida, H., Sakamoto, T., Aoki, K., et al. (2003). Microbial communities associated with geological horizons in coastal subseafloor sediments from the sea of Okhotsk. *Appl. Environ. Microbiol.* 69 (12), 7224–7235. doi: 10.1128/AEM.69.12.7224-7235.2003

Jing, H., Wang, R., Jiang, Q., Zhang, Y., and Peng, X. (2020). Anaerobic methane oxidation coupled to denitrification is an important potential methane sink in deep-sea cold seeps. *Sci. Total Environ.* 748, 142459. doi: 10.1016/j.scitotenv.2020.142459

Kemp, P. F., and Aller, J. Y. (2004). Estimating prokaryotic diversity: When are 16S rDNA libraries large enough? *Limnology Oceanography-Methods* 2, 114–125. doi: 10.4319/lom.2004.2.114

Kong, J., Feng, J., Sun, L., and Zhang, S. (2023). Evaluating the reproducibility of amplicon sequencing data derived from deep-sea cold seep sediment-associated microbiota. *Microbiol. Spectr.* 11 (3), e04048–e04022. doi: 10.1128/spectrum.04048-22

Lee, D.-H., Kim, J.-H., Lee, Y. M., Kim, J.-H., Jin, Y. K., Paull, C., et al. (2021). Geochemical and microbial signatures of siboglinid tubeworm habitats at an active mud volcano in the Canadian Beaufort Sea. *Front. Mar. Sci.* 8. doi: 10.3389/fmars.2021.656171

Legendre, P., Fortin, M.-J., and Borcard, D. (2015). Should the Mantel test be used in spatial analysis? *Methods Ecol. Evol.* 6 (11), 1239–1247. doi: 10.1111/2041-210x.12425

Leprich, D. J., Flood, B. E., Schroedl, P. R., Ricci, E., Marlow, J. J., Girguis, P. R., et al. (2021). Sulfur bacteria promote dissolution of authigenic carbonates at marine methane seeps. *ISME J.* 15 (7), 2043–2056. doi: 10.1038/s41396-021-00903-3

Li, X., Dai, Z., Di, P., Feng, J., Tao, J., Chen, D., et al. (2021). Distinct bottom-water bacterial communities at methane seeps with various seepage intensities in Haima, South China Sea. *Front. Mar. Sci.* 8. doi: 10.3389/fmars.2021.753952

Li, J. W., Peng, X. T., Bai, S. J., Chen, Z. Y., and Van Nostrand, J. D. (2018a). Biogeochemical processes controlling authigenic carbonate formation within the sediment column from the Okinawa Trough. *Geochimica Et Cosmochimica Acta* 222, 363–382. doi: 10.1016/j.gca.2017.10.029

Li, N., Yang, X., Peng, J., Zhou, Q., and Chen, D. (2018b). Paleo-cold seep activity in the southern South China Sea: Evidence from the geochemical and geophysical records of sediments. *J. Asian Earth Sci.* 168, 106–111. doi: 10.1016/j.jseaes.2017.10.022

Li, H., Yang, Q., and Zhou, H. (2020). Niche differentiation of sulfate- and iron-dependent anaerobic methane oxidation and methylotrophic methanogenesis in deep sea methane seeps. *Front. Microbiol.* 11. doi: 10.3389/fmicb.2020.01409

Ling, J., Guan, H., Liu, L., Tao, J., Li, J., Dong, J., et al. (2020). The diversity, composition, and putative functions of gill-associated bacteria of bathymodiolin mussel and vesicomyid clam from haima cold seep, South China Sea. *Microorganisms* 8 (11), 1699. doi: 10.3390/microorganisms8111699

Liu, C., Han, K., Lee, D.-J., and Wang, Q. (2016). Simultaneous biological removal of phenol, sulfide, and nitrate using expanded granular sludge bed reactor. *Appl. Microbiol. Biotechnol.* 100 (9), 4211–4217. doi: 10.1007/s00253-016-7293-2

Liu, W., Wu, Z., Xu, S., Wei, J., Peng, X., Li, J., et al. (2020). Pore-water dissolved inorganic carbon sources and cycling in the shallow sediments of the Haima cold seeps, South China Sea. *J. Asian Earth Sci.* 201, 104495. doi: 10.1016/j.jseaes.2020.104495

Marlow, J. J., Hoer, D., Jungbluth, S. P., Reynard, L. M., Gartman, A., Chavez, M. S., et al. (2021). Carbonate-hosted microbial communities are prolific and pervasive methane oxidizers at geologically diverse marine methane seep sites. *Proc. Natl. Acad. Sci.* 118 (25), e2006857118. doi: 10.1073/pnas.2006857118

Marlow, J. J., Steele, J. A., Ziebis, W., Thurber, A. R., Levin, L. A., and Orphan, V. J. (2014). Carbonate-hosted methanotrophy represents an unrecognized methane sink in the deep sea. *Nat. Commun.* 5 (1), 5094. doi: 10.1038/ncomms6094

Naehr, T. H., Eichhubl, P., Orphan, V. J., Hovland, M., Paull, C. K., Ussler, W., et al. (2007). Authigenic carbonate formation at hydrocarbon seeps in continental margin sediments: A comparative study. *Deep Sea Res. Part II: Topical Stud. Oceanography* 54 (11), 1268–1291. doi: 10.1016/j.dsr2.2007.04.010

Niemann, H., Lösekann, T., de Beer, D., Elvert, M., Nadalig, T., Knittel, K., et al. (2006). Novel microbial communities of the Haakon Mosby mud volcano and their role as a methane sink. *Nature* 443 (7113), 854–858. doi: 10.1038/nature05227

Niu, M., Fan, X., Zhuang, G., Liang, Q., and Wang, F. (2017). Methane-metabolizing microbial communities in sediments of the Haima cold seep area, northwest slope of the South China Sea. *FEMS Microbiol. Ecol.* 93 (9). doi: 10.1093/femsec/fix101

Nöthen, K., and Kasten, S. (2011). Reconstructing changes in seep activity by means of pore water and solid phase Sr/Ca and Mg/Ca ratios in pockmark sediments of the Northern Congo Fan. *Mar. Geology* 287 (1), 1–13. doi: 10.1016/j.margeo.2011.06.008

Núñez-Useche, F., Canet, C., Liebetrau, V., Puig, T. P., Ponciano, A. C., Alfonso, P., et al. (2018). Redox conditions and authigenic mineralization related to cold seeps in central Guaymas Basin, Gulf of California. *Mar. Petroleum Geology* 95, 1–15. doi: 10.1016/j.marpetgeo.2018.04.010

Offre, P., Spang, A., and Schleper, C. (2013). Archaea in biogeochemical cycles. *Annu. Rev. Microbiol.* 67 (1), 437–457. doi: 10.1146/annurev-micro-092412-155614

Orcutt, B., Boetius, A., Elvert, M., Samarkin, V., and Joye, S. B. (2005). Molecular biogeochemistry of sulfate reduction, methanogenesis and the anaerobic oxidation of methane at Gulf of Mexico cold seeps. *Geochimica Cosmochimica Acta* 69 (17), 4267–4281. doi: 10.1016/j.gca.2005.04.012

Pierre, C., Demange, J., Blanc-Valleron, M.-M., and Dupré, S. (2017). Authigenic carbonate mounds from active methane seeps on the southern Aquitaine Shelf (Bay of Biscay, France): Evidence for anaerobic oxidation of biogenic methane and submarine groundwater discharge during formation. *Continental Shelf Res.* 133, 13–25. doi: 10.1016/j.csr.2016.12.003

Roberts, H. H., Feng, D., and Joye, S. B. (2010). Cold-seep carbonates of the middle and lower continental slope, northern Gulf of Mexico. *Deep Sea Res. Part II: Topical Stud. Oceanography* 57 (21), 2040–2054. doi: 10.1016/j.dsr2.2010.09.003

Rognes, T., Flouri, T., Nichols, B., Quince, C., and Mahe, F. (2016). VSEARCH: a versatile open source tool for metagenomics. *Peerj* 4, e2584. doi: 10.7717/peerj.2584

Sun, Y., Wang, M., Zhong, Z., Chen, H., Wang, H., Zhou, L., et al. (2022). Adaption to hydrogen sulfide-rich environments: Strategies for active detoxification in deep-sea symbiotic mussels, Gigantidas platifrons. *Sci. Total Environ.* 804, 150054. doi: 10.1016/j.scitotenv.2021.150054

Takahashi, S., Tomita, J., Nishioka, K., Hisada, T., and Nishijima, M. (2014). Development of a prokaryotic universal primer for simultaneous analysis of bacteria and archaea using next-generation sequencing. *PloS One* 9 (8), e105592. doi: 10.1371/journal.pone.0105592

Thomas, T. R. A., Das, A., and Adikesavan, L. P. (2018). A review on the phylogeography of potentially chemoautotrophic bacteria from major vent and seep fauna and their contribution to primary production. *Geomicrobiology J.* 35 (7), 612–634. doi: 10.1080/01490451.2018.1440035

Valentine, D. L., Kastner, M., Wardlaw, G. D., Wang, X., Purdy, A., and Bartlett, D. H. (2005). Biogeochemical investigations of marine methane seeps, Hydrate Ridge,

Oregon. *J. Geophysical Research: Biogeosciences* 110 (G2), G02005. doi: 10.1029/2005JG000025

Wei, J., Wu, T., Zhang, W., Deng, Y., Xie, R., Feng, J., et al. (2020). Deeply buried authigenic carbonates in the qiongdongnan basin, South China Sea: implications for ancient cold seep activities. *Minerals* 10 (12), 1135. doi: 10.3390/min10121135

Wei, Z., Xu, T., Shang, S., Tian, H., Cao, Y., Wang, J., et al. (2021). Laboratory experimental study on the formation of authigenic carbonates induced by microbes in marine sediments. *J. Mar. Sci. Eng.* 9 (5), 479. doi: 10.3390/jmse9050479

Willis, A. D. (2019). Rarefaction, alpha diversity, and statistics. *Front. Microbiol.* 10. doi: 10.3389/fmicb.2019.02407

Xin, Y., Wu, N., Sun, Z., Wang, H., Chen, Y., Xu, C., et al. (2022). Methane seepage intensity distinguish microbial communities in sediments at the Mid-Okinawa Trough. *Sci. Total Environ.* 851, 158213. doi: 10.1016/j.scitotenv.2022.158213

Xu, H., Du, M., Li, J., Zhang, H., Chen, W., Wei, J., et al. (2020). Spatial distribution of seepages and associated biological communities within Haima cold seep field, South China Sea. *J. Sea Res.* 165, 101957. doi: 10.1016/j.seares.2020.101957

Yilmaz, P., Parfrey, L. W., Yarza, P., Gerken, J., Pruesse, E., Quast, C., et al. (2013). The SILVA and "All-species Living Tree Project (LTP)" taxonomic frameworks. *Nucleic Acids Res.* 42 (D1), D643–D648. doi: 10.1093/nar/gkt1209

Zhang, Y., Su, X., Chen, F., Wang, Y., Jiao, L., Dong, H., et al. (2012). Microbial diversity in cold seep sediments from the northern South China Sea. *Geosci. Front.* 3 (3), 301–316. doi: 10.1016/j.gsf.2011.11.014

Zhang, Q., Wu, D., Jin, G., Mao, S., Liu, J., Yang, C., et al. (2022a). Novel use of unique minerals to reveal an intensified methane seep during the last glacial period in the South China Sea. *Mar. Geology* 452, 106901. doi: 10.1016/j.margeo.2022.106901

Zhang, Q., Wu, D., Jin, G., Xu, X., Yang, C., and Liu, L. (2022b). Methane seep in the Shenhu area of the South China sea using geochemical and mineralogical features. *Mar. Petroleum Geology* 144, 105829. doi: 10.1016/j.marpetgeo.2022.105829

Zhou, J., Bruns, M. A., and Tiedje, J. M. (1996). DNA recovery from soils of diverse composition. *Appl. Environ. Microbiol.* 62 (2), 316–322. doi: 10.1128/aem.62.2.316-322.1996

Zhuang, G.-C., Xu, L., Liang, Q., Fan, X., Xia, Z., Joye, S. B., et al. (2019). Biogeochemistry, microbial activity, and diversity in surface and subsurface deep-sea sediments of South China Sea. *Limnology Oceanography* 64 (5), 2252–2270. doi: 10.1002/lno.11182